

Steady-state Power Flow Model of Energy Router Embedded AC Network and Its Application in Optimizing Power System Operation

Jianqiang Miao, *Student Member, IEEE*, Ning Zhang, *Member, IEEE*,
Chongqing Kang, *Fellow, IEEE*, Jianxiao Wang, *Student Member, IEEE*,
Yi Wang, *Student Member, IEEE*, and Qing Xia, *Senior Member, IEEE*

Abstract-- The energy router is an emerging device concept that is based on an advanced power electronic technique. It is able to realize flexible and dynamic electric power distribution in power systems analogous to the function of information routers in the Internet. It is of great interest to investigate how the energy router can be used to optimize power system operation. This paper formulates the steady-state power flow model of the energy router embedded system network and the related optimal power flow (OPF) formulation. The role of the energy router in providing extra flexibility to optimize the system operation is studied. Case studies are carried out on a modified IEEE RTS-79 system and a modified IEEE 118 bus system with the energy router. The results show that the energy router is able to optimize the operation of the power system through controlling the power injections and voltage of ports of the energy router. Operating objective such as adjusting branch power flow, improving bus voltage and reducing active power losses of the grid can be reached under different objective functions.

Index Terms-- energy router, optimal power flow, energy internet, flexibility, AC/DC

NOMENCLATURE

Sets and Indices

- S_N Set of buses of the AC network
- S_K Set of ports of the energy router
- i Index for AC buses, $i \in S_N$
- l Index for energy router ports, $l \in S_K$
- N Number of buses of the AC network
- K Number of ports of the energy router
- Φ Primary side of the energy router
- Ψ Secondary side of the energy router

Parameters

- G^H Port conductance of the energy router
- B^H Port admittance of the energy router
- B_c^H Ground admittance of ports of the energy router

Variables

- P Active power injections of the AC network
- Q Reactive power injections of the AC network
- U Voltage magnitudes of the AC network
- θ Voltage angles of the AC network
- P^H Active power injection of the energy router
- Q^H Reactive power injection of the energy router
- m Equivalent utility control factor
- E Voltage at the DC side of ports of the energy router
- δ Voltage angle lags of ports of the energy router
- E_Φ Normalized DC voltage of the primary side of the energy router
- E_Ψ Normalized DC voltage of the secondary side of the energy router

Matrices

- \mathbf{M} Port-bus incidence matrix
- \mathbf{G} Conductance matrix
- \mathbf{B} Admittance matrix

I. INTRODUCTION

WITH the rapid development of power electronic and communication technologies, flexible power electronic devices are continuing to change the power system [1]. The rapidly increasing renewable energy integration and smart grid participators (e.g., distributed generation, electric vehicles and distributed storage) have increased the need for smarter energy management [2][3]. The concept of energy routers is therefore proposed, which is defined as a series of power electronic equipment that is able to manage energy flows as flexibly as information flows in the Internet [4]. It is considered an enabling component for building the future form of the smart grid: the energy internet [5] [6].

There has been some preliminary research on energy routers, covering their functionality, architecture design, and control strategies. The definitions and configurations of energy routers are distinct. However, visions of their functionality are similar. The power flow on each feeder can be flexibly controlled in both directions and can be regulated in real time [7]. The voltage of each feeder can be independently controlled to optimize the performance of the overall system [8]. The energy router facilitates distributed renewable energy resources and storage devices accessing and

This work was supported jointly by Major International (Regional) Joint Research Project of National Science Foundation of China (No. 51620105007) and National Natural Science Funds for Distinguished Young Scholar (No. 51325702)

J. Miao, N. Zhang, C. Kang, J. Wang, Y. Wang and Q. Xia are with the State Key Lab of Power Systems, Department of Electrical Engineering, Tsinghua University, Beijing 100084, China. (Corresponding author: Chongqing Kang, e-mail: cqkang@tsinghua.edu.cn).

detaching from the power system freely, forming plug-and-play energy ports [9]. The energy router is also able to isolate the faults of the distribution system [10]. Working together with the energy storage devices, energy routers are able to shift the energy consumption from one period to another flexibly [11]. Furthermore, energy routers are able provide dynamic control to support the security and stability of the power system through situational awareness techniques [12].

At present, research on the energy router is mainly concentrated on its inner power electronic configuration. The project on the Future Renewable Electric Energy Delivery and Management System (FREEDM) carried out by North Carolina State University is designing a solid-state-transformer-based (SST-based) version of the energy router for the purposes of developing a smart distribution network and micro grid [13]. The energy router is also equipped with intelligent communications that facilitate the smart control of both loads and generators in the distribution network or micro grid [4]. Researchers have reported different power electronic topologies for energy routers [14] - [16]. With the appropriate control strategies for power electronics, the power output/injection can be independently controlled to meet consumers' demands [17] [18]. Using the energy router as a basic element, the distribution system can achieve smarter energy management and improve the performance of the energy internet [19] [20].

The functionality of the energy router in optimizing the operation of power systems has received great attention [21] - [23]. A generalized system connection diagram of an SST-based energy router is shown in Fig. 1. The energy router connects two or more layers of the power system or connects a micro grid to the power grid. The energy router usually has multiple ports that could be connected to different buses or feeders [24]. Through such layouts, the energy router is able to improve the power system operation using strategic controls: 1) By optimizing the power output/injections of ports on the same levels of power grids, the power flows on each layer of the grid can be optimized to reduce congestion [25]. 2) By optimizing the power flow through the SST, the power flow through other conventional transformers can also be changed to eliminate congestion. 3) By independently setting the bus voltage of the associated ports, the power system reactive power flows can be optimized to reduce losses [26]. 4) By intelligently controlling the operation of the micro grid, the efficiency of the entire power system can be improved [27].

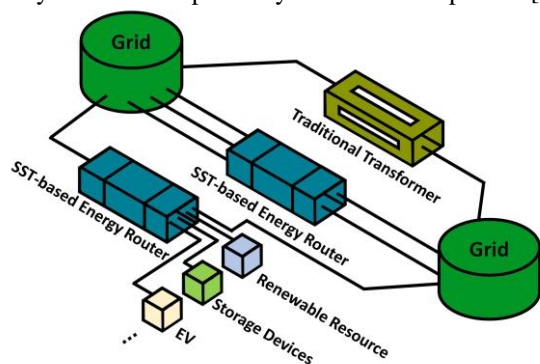


Fig. 1. System connection diagram with the participation of energy routers

In addition to the energy router's inner structural design, component-level simulations and control strategies, research at the power system level is also of great value, e.g., how the energy router can be used to improve the power system operation and how much benefit it can bring to the power system. Our latest work addresses this issue by proposing a generalized configuration of the SST-based energy router [28]. The steady-state model of the energy router is derived based on the circuit equations of the power electronics. The steady-state model acts as a basic formulation for the power flow calculations and optimizations considering energy routers.

Current research on the energy router is focused on the low voltage level (10 kV/400 V), and its future application in the transmission network is expected to be feasible and valuable: 1) The technology needed for high-voltage, high-capacity energy routers is already in the demonstration stage. Voltage-Sourced Converters (VSC) for the transmission level have been used in real power systems, e.g., the Unified Power Flow Controller (UPFC) in Jiangsu province, China [29] and the Zhoushan DC grid in China [30]. The technique of SST-related power electronics is also able to reach higher voltage levels by cascading multiple modules; for example, the State Grid Corporation of China is building a multi-port DC network at Zhangbei Test Base [31]. 2) The energy router in the transmission grid is able to play a more effective role in controlling the power flow than in the distribution network. By strategically routing the energy, it is able to adjust the power flow in both voltage levels, thereby improving the operation state of the power system.

On this basis, this paper proposes the OPF formulation of power systems equipped with an energy router. Because the energy router is able to change the network power flow by setting the related voltage and power injections, compared with the conventional OPF problem [32], the energy router provides extra flexibility in controlling the power system. The proposed OPF model helps explore how the control of the energy router can be optimized together with the output of generators and the load tap changers of transformers. To solve such a nonconvex, nonlinear programming model [33], the tool *IPOPT* is applied [34]. The gradient of the objective functions and the Jacobian matrix of the constraints are derived for using the *IPOPT* solver [35]. The results of the OPF model under different optimal targets with and without the energy router are compared to demonstrate the role of the energy router in improving the performance of the overall system.

The contributions of this paper are summarized as follows:

- 1) We propose a normalized power flow model for an energy-router-incorporated power system, which has not been studied yet, by defining the port-bus incidence matrix;
- 2) The OPF model of the energy router embedded power system is proposed, thus facilitating an optimization of the operating state of the power system via the coordination of generators, transformers, and the energy router;
- 3) Effects of the energy router on improving the

performance of power systems are demonstrated by running OPF model under different operating objectives.

The remainder of the paper is organized as follows. Section II outlines the generalized steady-state mathematical model of the energy router and derives the network power flow equations for a power system with the energy router. The OPF formulation with the participation of the energy router is proposed in Section III. Section IV carries out preliminary case studies by a modified IEEE RTS-79 system and a modified IEEE 118 bus system, comparing the results of the OPF formulation under different optimization objectives and the results between the OPF formulation and normal system operating states. Finally, Section V concludes this paper.

II. POWER FLOW MODEL OF THE ENERGY ROUTER INCORPORATED POWER SYSTEM

A. Configuration of the Energy Router

The configuration of the generalized energy router is shown in Fig. 2. It consists of two sides (voltage levels): the primary side (with subscript Φ) and the secondary side (with subscript Ψ). Each side can be placed with several ports, e.g., K_Φ ports for the primary side and K_Ψ for the secondary side. Each port is made of a flexible AC/DC converter that releases or extracts power from the DC bus. The two DC buses are linked using a DC/DC transformer. The proposed configuration can be easily expanded to multiple voltage levels.

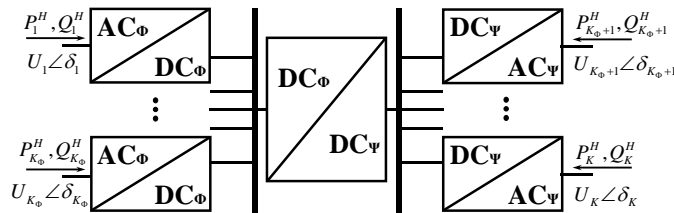


Fig. 2. Configuration of the generalized energy router

In the generalized configuration of the energy router, the active and reactive injection power of each port are expressed by P^H and Q^H , respectively, and the magnitude and angle of the port voltage are expressed by U and δ , respectively. The primary side has K_Φ ports in total, which share the same DC voltage E_Φ , as does the secondary side. The parameters on the AC grid side P^H , Q^H , and U of each port can be independently controlled by the flexible VSC-based AC/DC converter.

B. Power Flow Equations of the Energy Router

The equivalent circuit mode of the AC/DC converter is shown in Fig. 3 [36]. For the l -th port, the converter is composed of a converter bridge, a converter reactor, a DC capacitor and an AC filter. The fundamental wave voltage is marked by U_l^H , and δ_l denotes the angle by which U_l^H lags U_l . The loss of the converter is described by resistance R_l^H , whereas X_l^H and X_{cl}^H represent reactance at the fundamental frequency of the converter and filter, respectively.

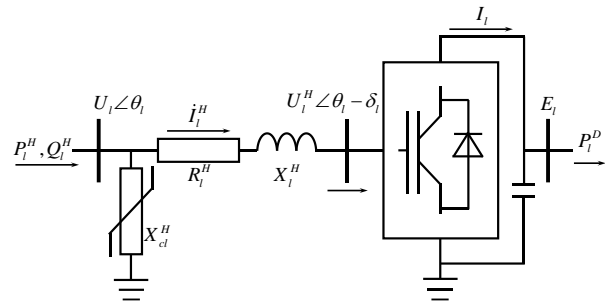


Fig. 3. Model of the AC/DC converter of the energy router

The conductance and susceptance of the AC/DC converter at each port are defined in (1).

$$\begin{aligned} G_l^H &= \frac{R_l^H}{(R_l^H)^2 + (X_l^H)^2} \\ B_l^H &= -\frac{X_l^H}{(R_l^H)^2 + (X_l^H)^2} \\ B_{cl}^H &= -\frac{1}{X_{cl}^H} \end{aligned} \quad (1)$$

The power flow equation of the l -th port of the energy router can be expressed as

$$P_l^H - G_l^H U_l^2 + m_l E_l (G_l^H \cos \delta_l + B_l^H \sin \delta_l) U_l = 0 \quad (2)$$

$$Q_l^H + (B_{cl}^H + B_l^H) U_l^2 + m_l E_l (G_l^H \sin \delta_l - B_l^H \cos \delta_l) U_l = 0 \quad (3)$$

In (2) and (3), U_l refers to the voltage magnitude of the bus in the AC network, which connects to the l -th port of the energy router, and m_l is the defined equivalent utility control factor, which is the ratio of the AC side voltage magnitude and the DC side voltage magnitude of the port of the energy router, which means:

$$U_l^H = m_l E_l \quad (4)$$

where U_l^H and E_l are the related voltage magnitudes that are pointed out in Fig. 3. The equivalent utility control factor is determined by the voltage utilization factor of the DC side (μ) and the modulation index of the converters (Λ). The voltage utilization factor of the DC side and the modulation index of the converters are common control parameters in power electronics. For the VSC-based AC/DC converter, the voltage utilization factor of the DC side denotes the maximum ratio of the AC voltage fundamental amplitude to the DC side voltage. The modulation index is the ratio of the modulation wave voltage amplitude to the carrier wave voltage amplitude In Pulse-Width Modulation (PWM). The quantitative relationship of m_l , μ_l and Λ_l can be expressed as follows:

$$m_l = \frac{\mu_l \Lambda_l}{\sqrt{2}} \quad (5)$$

Equation (5) shows that a larger voltage utilization factor of the DC side and a smaller modulation index of the converter will result in a larger utility control factor.

The active power balance equation of the energy router is described as

$$\left(\sum_{l \in K} E_l I_l \right) - \left(\sum_{l \in K_\Phi} I_l \right)^2 R_\Phi - \left(\sum_{l \in K_\Psi} I_l \right)^2 R_\Psi - \Delta P_{st} = 0 \quad (6)$$

where ΔP_{st} represents the static power loss of the DC/DC transformer, the loss of the DC/DC transformer is represented by equivalent resistance R_Φ (the primary side) and R_Ψ (the secondary side). In (6), I_l is defined as

$$I_l = -G_l^H m_l^2 E_l + m_l (G_l^H \cos \delta_l - B_l^H \sin \delta_l) U_l \quad (7)$$

for all $l \in S_K$.

C. Port-bus Incidence Matrix

To integrate the power flow model of the energy router into the classic power flow model, the port-bus incidence matrix M is introduced. M is an $N \times K$ matrix, the elements of which are defined as follows

- 1) M_{il} is 1 if the i -th bus of the AC network is connected to the l -th port of the energy router;
- 2) M_{il} is 0 in other cases.

D. Normalized Power Flow Model

By introducing the port-bus incidence matrix, the normalized power flow model for the energy router-incorporated power system can be built as follows:

$$P_{gi} - P_{di} - \sum_{l=1}^K M_{il} P_l^H - U_i \sum_{j=1}^N U_j (B_{ij} \sin \theta_{ij} + G_{ij} \cos \theta_{ij}) = 0 \quad (8)$$

$$Q_{gi} - Q_{di} - \sum_{l=1}^K M_{il} Q_l^H - U_i \sum_{j=1}^N U_j (G_{ij} \sin \theta_{ij} - B_{ij} \cos \theta_{ij}) = 0 \quad (9)$$

for all $i \in S_N$, and

$$P_l^H - G_l^H \sum_{i=1}^N M_{il} U_i^2 \quad (10)$$

$$+ m_l E_l (G_l^H \cos \delta_l + B_l^H \sin \delta_l) \sum_{i=1}^N M_{il} U_i = 0$$

$$Q_l^H + (B_{cl}^H + B_l^H) \left(\sum_{i=1}^N M_{il} U_i^2 \right) \quad (11)$$

$$+ m_l E_l (-B_l^H \cos \delta_l + G_l^H \sin \delta_l) \sum_{i=1}^N M_{il} U_i = 0$$

for all $l \in S_K$.

Furthermore, (7) can be reorganized as

$$I_l = -G_l^H m_l^2 E_l + m_l (G_l^H \cos \delta_l - B_l^H \sin \delta_l) \sum_{i=1}^N M_{il} U_i \quad (12)$$

Equations (8) - (11), together with (6) and (12), form the power flow equations of the overall system network, which is used as a basis in formulating the OPF model in the next section.

III. OPF FORMULATION CONSIDERING ENERGY ROUTER

A. Objective Functions

The purpose of this integrated OPF model is to optimize the output power for all generators and the port power flow of the energy router during operation. In this formulation, bus power injections, bus states, and control and state variables of the

energy router are modified coordinately, aiming to achieve the ideal operating state of the power system.

Objective functions under different control targets are shown below, respectively.

- 1) Minimize system active power losses

$$\text{Min } F_1 = \sum_{i=1}^N (P_{g_i} - P_{d_i}) \quad (13)$$

- 2) Minimize generation costs

$$\text{Min } F_2 = \sum_{i=1}^N C_i(P_{g_i}) \quad (14)$$

Usually, quadratic functions are commonly used to describe the generation costs, which can be expressed as

$$C_i(P_{g_i}) = \alpha_i P_{g_i}^2 + \beta_i P_{g_i} + \gamma_i \quad (15)$$

- 3) Minimize bus voltage deviation

$$\text{Min } F_3 = \sum_{i=1}^N (U_i - U_{i0})^2 \quad (16)$$

B. Constraints

This formulation is subject to the following constraints:

- 1) Power flow equations for the AC network

$$\Delta P_{gi} = 0 \quad (17)$$

$$\Delta Q_{gi} = 0 \quad (18)$$

for all $i \in S_N$. ΔP_{gi} and ΔQ_{gi} are defined by (8) and (9), respectively.

- 2) Line power flow upper and lower bound constraints of the AC network

$$S_{ij}^{\min} \leq S_{ij} = U_i U_j (G_{ij} \cos \theta_{ij} + B_{ij} \sin \theta_{ij}) - G_{ij} U_i^2 \leq S_{ij}^{\max} \quad (19)$$

for all $i, j \in S_N$.

- 3) Port power flow equations of the energy router

$$\Delta P_l^H = 0 \quad (20)$$

$$\Delta Q_l^H = 0 \quad (21)$$

for all $l \in S_K$. ΔP_l^H and ΔQ_l^H are defined by (10) and (11), respectively.

- 4) Voltage balance equations of the DC/DC level

For all variables on the primary side of the energy router, we have

$$\Delta E_l = E_l - E_\Phi = 0, \text{ for all } l \in S_{K_\Phi} \quad (22)$$

And for all variables on the secondary side of the energy router, we have

$$\Delta E_l = E_l - E_\Psi = 0, \text{ for all } l \in S_{K_\Psi} \quad (23)$$

- 5) Active power balance equation of the energy router

$$\Delta P_{loss} = 0 \quad (24)$$

in (24), ΔP_{loss} is defined by (6) and (7).

- 6) DC/DC level exchanged power flow upper and lower bound constraints of the energy router

$$P_{DC\Phi}^{\min} \leq P_{DC\Phi} = E_\Phi \sum_{l \in K_\Phi} (-G_l^H m_l^2 E_\Phi + f(l)) \leq P_{DC\Phi}^{\max} \quad (25)$$

$$P_{DC\Psi}^{\min} \leq P_{DC\Psi} = E_\Psi \sum_{l \in K_\Psi} (-G_l^H m_l^2 E_\Psi + f(l)) \leq P_{DC\Psi}^{\max} \quad (26)$$

where

$$f(l) = m_l \left(G_l^H \cos \delta_l + B_l^H \sin \delta_l \right) \sum_{i=1}^N M_{il} U_i \quad (27)$$

7) Port complex power upper and lower bound constraints of the energy router

$$0 \leq S_l^{H2} = \left(P_l^H \right)^2 + \left(Q_l^H \right)^2 \leq \left(S_l^{H,\max} \right)^2, \text{ for all } l \in S_K \quad (28)$$

8) Upper and lower bounds of the parameters involved in this model

$$P_i^{\min} \leq P_i \leq P_i^{\max}, \text{ for all } i \in S_N \quad (29)$$

$$Q_i^{\min} \leq Q_i \leq Q_i^{\max}, \text{ for all } i \in S_N \quad (30)$$

$$U_i^{\min} \leq U_i \leq U_i^{\max}, \text{ for all } i \in S_N \quad (31)$$

$$\theta_i^{\min} \leq \theta_i \leq \theta_i^{\max}, \text{ for all } i \in S_N \quad (32)$$

$$P_l^{H,\min} \leq P_l^H \leq P_l^{H,\max}, \text{ for all } l \in S_K \quad (33)$$

$$Q_l^{H,\min} \leq Q_l^H \leq Q_l^{H,\max}, \text{ for all } l \in S_K \quad (34)$$

$$E_l^{\min} \leq E_l \leq E_l^{\max}, \text{ for all } l \in S_K \quad (35)$$

$$\delta_l^{\min} \leq \delta_l \leq \delta_l^{\max}, \text{ for all } l \in S_K \quad (36)$$

$$m_l^{\min} \leq m_l \leq m_l^{\max}, \text{ for all } l \in S_K \quad (37)$$

The overall OPF formulation is discussed above. The optimization variables in this programming model include P , Q , U , θ , P^H , Q^H , E , δ and m . Among all of them, P , Q , P^H , Q^H , E and m are independent variables that can be optimized while the rest of the variables are determined by these independent variables.

C. Matrix Formulation of the Optimization Problem

To make the model more easily to be understood, the model is converted into a unified matrix formulation. The variables and constraints are first reorganized. The variables appearing in the OPF model are placed in a normalized vector form, namely

$$\mathbf{x} = \left[\mathbf{P}_g^T \ \mathbf{Q}_g^T \ \mathbf{U}^T \ \boldsymbol{\theta}^T \ (\mathbf{P}^H)^T \ (\mathbf{Q}^H)^T \ \mathbf{E}^T \ \boldsymbol{\delta}^T \ \mathbf{m}^T \ E_{\phi}^T \ E_{\psi}^T \right]^T \quad (38)$$

The constraints of the model are reorganized as

$$\mathbf{C} = \left[\Delta \mathbf{P}_{gi} \ \Delta \mathbf{Q}_{gi} \ \mathbf{S}_{ij} \ \Delta \mathbf{P}_i^H \ \Delta \mathbf{Q}_i^H \ \Delta \mathbf{E}_i \ \Delta P_{loss} \ \mathbf{P}_{DC} \ \mathbf{S}_i^{H2} \right]^T \quad (39)$$

in (39), \mathbf{C} represents the combination of constraints (17) - (28).

After the reorganization of the variables and constraints, the OPF model can be rewritten in a generalized form, which is described as

$$\text{Min } F(\mathbf{x}) \quad (40)$$

Subject to

$$\mathbf{C}_{\min} \leq \mathbf{C} \leq \mathbf{C}_{\max} \quad (41)$$

$$\mathbf{X}_{\min} \leq \mathbf{X} \leq \mathbf{X}_{\max} \quad (42)$$

The subsequent analysis and the simulation is carried out based on this normalized form.

D. Discussion

Incorporated with the energy router, the OPF model of the comprehensive system differs from the conventional model in the following aspects.

1) Optimization space

After the system has incorporated the energy router, new constraints are brought into the formulation. These constraints emerge mainly because of the port power flow and the inner power balance equations of the energy router. Without the energy router's participation, the constraints of the related buses and branches are in equality forms, and the value of power injections on the related buses and power flow in the related branches must follow Kirchhoff's voltage law and do not have the freedom to be optimized individually. However, in the new OPF model, these equality constraints no longer exist; instead, the newly introduced constraints include the total power balance of the energy router and the related parameters varying within certain limits. These newly introduced constraints, together with the power balance constraints of the AC network, define the variable space of the OPF model.

2) Solving complexity

Compared with the formulations of the original network power flow constraints, the degree of nonlinearity is much higher on the newly introduced constraint features of the energy router. This is particular prominent in (24), which consists of the quartic polynomial, quadratic terms, trigonometric terms and their coupling forms. Some optimization tools based on the simplex method, such as *CPLEX*, are unsuitable for solving such a difficult programming model. Also, current approximation or relaxation approaches of OPF to satisfy the *CPLEX*'s requirements may not be applicable to such a formulation because adding energy router may jeopardize the precondition of such approximation or relaxation. Therefore, here we use *IPOPT* to directly solve the model. Similar to traditional OPF model, using *IPOPT* will also face the convergence problem. However, in this paper we only focus on the modeling of the energy router. In order to tackle the convergence problem, the initial value is selected beforehand.

3) The role of the energy router in power system optimization

The application of the energy router changes the structure of the system; moreover, the relationship among the power flow injections and bus voltages are also changed. Some quantities that are dependent on the power flow injections in the conventional system, such as voltage and power flow, can be adjusted through the decouple control strategies of the energy router. For example, the port voltages of the energy router can be determined individually if we would like to keep them on their assigned value. The magnitude and direction of the power flow at each port could be controlled flexibly, if there are congestions on some transmission lines and the power flow of some ports are required to change their direction in order to eliminate the congestion. All of the above can be achieved under the set of power balance equations of the energy router.

IV. CASE STUDY

The OPF formulation of the system is solved using *IPOPT* 3.12 together with Matlab R2015b on a Windows 7-based PC with four threads clocking at 2.50 GHz and 8 GB of RAM.

A. IEEE RTS-79 System

In this section, a modified IEEE RTS-79 system is used to demonstrate the results of the OPF formulation on the energy-router-incorporated system network under different optimal objectives, and comparisons among them are discussed.

1) System Configuration

The configuration of the modified RTS-79 system is shown in Fig. 4. Transformers between buses #9 and #11 and between #10 and #12 are replaced by an energy router with two primary ports (1 and 2) and two secondary ports (3 and 4). The rated capacity of the energy router is 350 MVA, and the rated voltages of the primary and secondary side are 138 kV and 230 kV, respectively. The total load of the power system is 2850 MW. The output of the generators is extracted from the example files from ‘Case24_ieee_rts’ in Matpower version 5.1. The impedance parameters of the primary and secondary sides are $R = 0.00181$, $X = 0.0363$, and $X_c = -7.2617$, with a 100 MVA base capacity. The equivalent resistance of the DC/DC transformer stage is set to $R_{E\phi} = 0.000494$, $R_{E\psi} = 0.000494$, and the static active power loss is set to $\Delta P_{st} = 0.0412$.

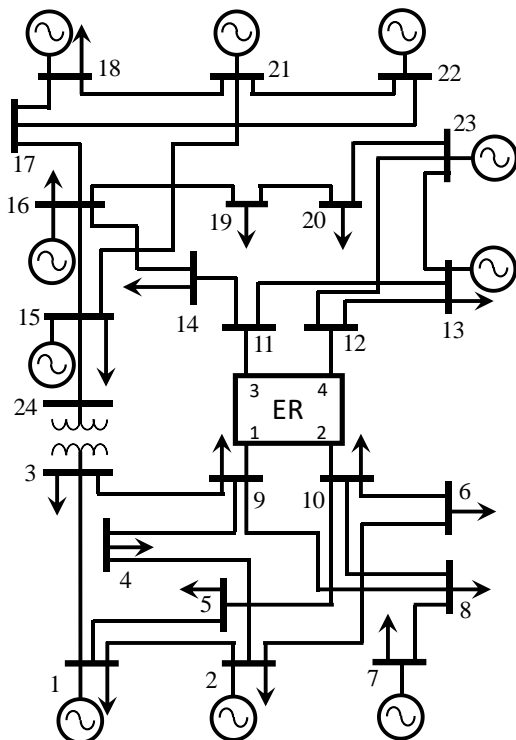


Fig. 4. Modified IEEE RTS-79 system with the energy router

2) General Experimental Results on Generation Data

The results of the modified IEEE RTS-79 system under different optimal targets proposed in Section III.A (F1, F2 and F3) are shown in this part. Fig. 5 shows the active and reactive generation outputs of the OPF results in these cases. Fig. 6 calculates the generation cost and the active power losses under different optimal objectives.

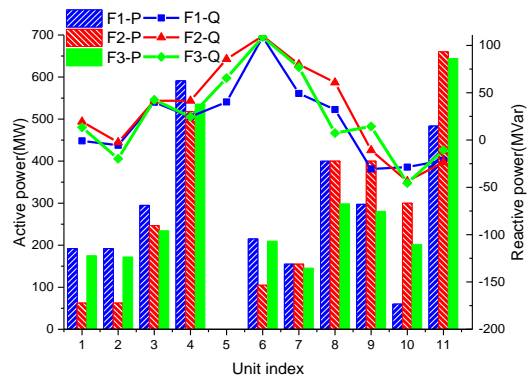


Fig. 5. System generation data of the OPF results

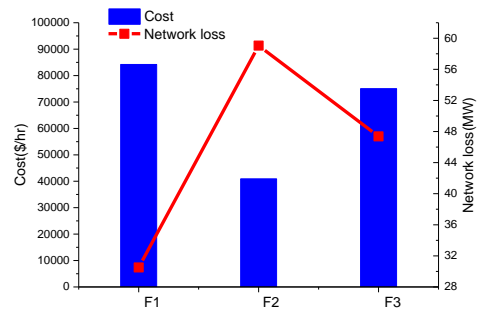


Fig. 6. Generation statistical information of the OPF results

Table I shows that the generation outputs vary under different optimal objectives, most of which reach their upper or lower bounds in each case. Table II shows that F2 has the lowest generation cost, whereas F1 has the minimum active power loss, agreeing with their respective control targets.

3) General Experiment Results on Operation States

The bus voltage magnitudes and angles of the OPF results are shown in Fig. 7. In the cases whose optimal targets are F1 and F2, the bus voltage magnitudes and angles are similar. The fluctuations among different buses are small in these two cases. Furthermore, in the last case with the minimum bus voltage deviation target (F3), the system bus voltages are very close to the rated value, which meets the optimal target.

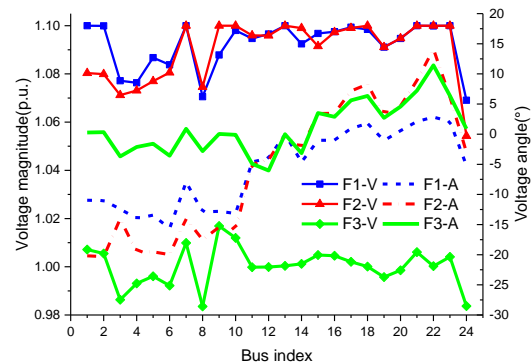


Fig. 7. Bus Voltage Magnitude and Angle of the OPF Results

A comparison between the above results shows that once the set targets are reached, other characteristics of the system must deviate from the normal value. In other words, it is impossible to achieve all benefits without bearing the related losses.

4) Discussion on the Functions of the Energy Router

Details of the inner operation information of the energy router in different cases are shown in Appendix A, including the active and reactive power injection of the energy router, equivalent utility control factor, voltage at the DC side of ports of the energy router and voltage angle lags of the ports of the energy router in the OPF results. It is meaningful to determine the differences in the energy-router-related buses and lines between the original system and the integrated system. Taking Case F2 as an example, Fig. 8 shows the port power flow injections of the energy router and the corresponding power injections in the original system under the objective of minimizing the system generation cost.

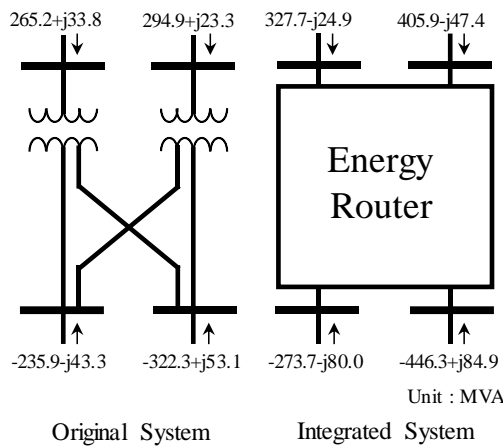


Fig. 8. Bus Voltage Angle of the OPF Results

The comparison in Fig. 8 shows that the energy router is able to change the power flow at the related ports. The values of the active and reactive power flow in the integrated case are much larger than they were in the conventional case. Thus, it would be easy to find the proper way to promote the system voltage level or operation states using this feature of the energy router.

B. IEEE 118 Bus System

In this part, the modified IEEE 118 bus system is used to compare the OPF results of the original system and the energy-router-incorporated system, under the optimal target of minimizing the system active power losses.

1) System Configuration

The parameters of the generator, nodes and branches are extracted from the example files from ‘Case118’ in Matpower version 5.1. The total load of the system is 4242 MW. The transformers of the original system, shown in Appendix B, are incorporated with an energy router with 9 ports on the primary side and 10 ports on the secondary side, of which the last port is connected to bus #10 in the original system. The rated capacity of the energy router is 500 MVA, and the rated voltage of the primary and secondary sides are 138 kV and 345 kV, respectively.

2) Experimental Results

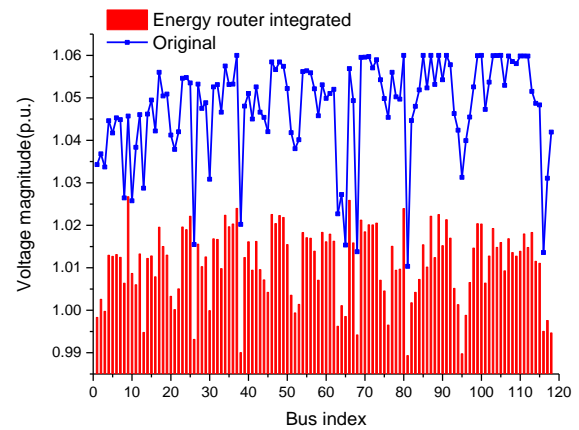


Fig. 9. Comparisons of the bus voltage magnitudes between the two cases

For the two cases, the total active power loss in the conventional system is 9.23 MW, whereas in the energy-router-incorporated system, the loss is 9.16 MW, slightly better. Moreover, the advantages are enhanced in other aspects after the energy router adjusts the system behavior. Fig. 9 demonstrates the comparisons of the bus voltage magnitudes between the systems. It is easy to find that the most voltage magnitudes decrease after the incorporation of the energy router. In the conventional case, many bus voltage magnitudes reach their upper bounds to lower the currents of the network, so the losses of the lines are reduced. However, in the modified system, the energy router is able to lower the system losses without pushing the bus voltage to the edge of the safety limit.

Fig. 10 compares the active power of each branch between the two cases. The results show that the energy router is able to manage the power flow of not only the branches that are directly connected to it but also those that it can indirectly impact. For example, the energy router lowers the power flow on branches #127 and #37 by 9.87 MW and 9.69 MW, respectively, and further shifts the power flow in branch #102 to branch #109. Because the branch has lower resistance, the active power losses are reduced. The results suggest that 1) the control of the energy router should consider not only the local region but the overall power system and 2) the location of the energy router determines how and how much it is able to improve the power system performance.

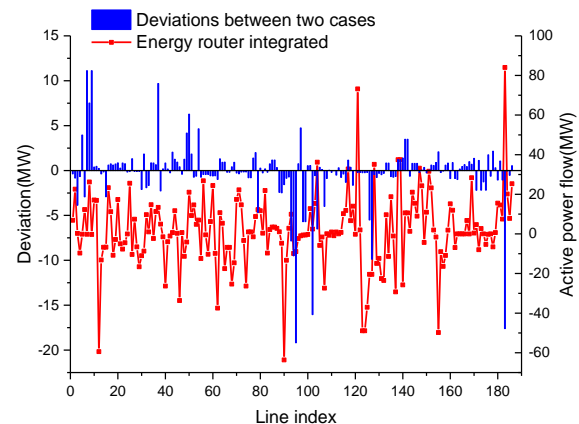


Fig. 10. Comparisons of the line active power flows between the two cases

3) Discussions

The purpose of the above comparisons between the original system and the energy router incorporated system is to validate the proposed model and conceptually demonstrate the how and how much the energy router improves the operation of the power system. It might be over-idealized compared to reality. In the real system operation, the practical control schemes may also need to be taken into consideration, such as the automatic voltage control scheme. Under such conditions, additional constraints may be introduced into this model to take into account more practical control schemes.

V. CONCLUSION

This paper proposes a generalized steady-state model of the energy router and expands the system power flow model by incorporating the formulation of the energy router using the port-bus incidence matrix. The energy router embedded OPF formulation is then proposed. The results of the case studies on a modified IEEE RTS-79 and a modified IEEE 118 bus system show that the system is able to optimize the power system operation through controlling the power injections and voltage of ports of the energy router. This study demonstrates the roles of the energy router in improving the performance of a power system in a smarter and more flexible manner (as an energy internet). It is of great value to further investigate the issues of system planning considering the energy router. For example, how the configuration of the energy router can be optimized with respect to the capacity of inverters on each port and the capacity of the SST from the power system point of view? Where and how many energy routers should be placed in the power system? The generalized mathematical steady-state model of the energy router and the OPF formulation of the energy-router-incorporated system network will act as the basic formulations for answering these questions.

APPENDIX A

TABLE A I. PORT DATA OF THE ENERGY ROUTER UNDER CASE F1

Port No	P ^H / MW	Q ^H / MW	E	δ/°	m
1	-199.1	-57.1	1.9	-3.41	0.5825
2	-294.1	75.4	1.9	-5.26	0.5668
3	199.4	-16.0	2.1	3.47	0.5206
4	302.4	-21.8	2.1	5.24	0.5228

TABLE A II. PORT DATA OF THE ENERGY ROUTER UNDER CASE F2

Port No	P ^H / MW	Q ^H / MW	E	δ/°	m
1	-273.7	-80.0	1.9	-4.54	0.5942
2	-446.3	85.0	1.9	-7.90	0.5706
3	327.7	-25.0	2.1	5.68	0.5232
4	406.0	-47.4	2.1	7.00	0.5275

TABLE A III. PORT DATA OF THE ENERGY ROUTER UNDER CASE F3

Port No	P ^H / MW	Q ^H / MW	E	δ/°	m
1	-484.2	-46.0	1.9	-10.26	0.5318
2	-486.1	200.0	1.9	-13.64	0.4468
3	500.0	200.0	2.1	13.57	0.3979
4	500.0	153.9	2.1	13.54	0.4033

TABLE A IV. PORT DATA OF THE ENERGY ROUTER UNDER CASE F4

Port No	P ^H / MW	Q ^H / MW	E	δ/°	m
1	-307.2	-69.6	1.96	-5.95	0.5336
2	-361.1	56.6	1.95	-7.50	0.5125

3	249.1	-27.1	2.05	5.18	0.4897
4	432.9	-70.9	2.06	8.88	0.4976

APPENDIX B

TABLE B I. TRANSFORMERS MODIFICATION INFORMATION OF THE IEEE 118 BUS SYSTEM

Transformer No	Associated bus No. of the primary side	Associated bus No. of the secondary side
1	5	8
2	25	26
3	17	30
4	37	38
5	59	63
6	61	64
7	66	65
8	69	68
9	80	81

REFERENCES

- [1] J. Rifkin, *The third industrial revolution: how lateral power is transforming energy, the economy, and the world*. New York: Palgrave MacMillan, 2011.
- [2] Z. Amjadi and S. S. Williamson, "Power-electronics-based solutions for plug-in hybrid electric vehicle energy storage and management systems," *IEEE Trans. Ind. Electron.*, vol. 57, no. 2, pp. 608 - 616, Feb. 2010.
- [3] Z. Bo, X. Lin, Q. Wang, Y. Yi, F. Zhou "Developments of power system protection and control". *Protection and Control of Modern Power Systems* vol. 1, pp. 1-8, 2016.
- [4] A. Huang, M. Crow, G. Heydt, J. Zheng, and S. Dale, "The future renewable electric energy delivery and management (FREEDM) system: the energy internet," *Proc. IEEE*, vol. 99, no. 1, pp.133 - 148, 2011
- [5] Y. Xu, J. Zhang, W. Wang, A. Juneja, and S. Bhattacharya, "Energy router: architectures and functionalities toward energy internet," in *Proc. 2011 IEEE Smart Grid Communications Conference*, pp 31 - 36
- [6] J. Zhang, W. Wang, and S. Bhattacharya, "Architecture of solid state transformer-based energy router and models of energy traffic," in *Innovative Smart Grid Technologies (ISGT), 2012 IEEE PES*, Jan. 2012, pp. 1 - 8.
- [7] X. She, F. Wang, R. Burgos, and A. Huang, "Solid state transformer interfaced wind energy system with integrated active power transfer, reactive power compensation and voltage conversion functions," *Energy Conversion Congress and Exposition (ECCE)*, 2012
- [8] X. She and A. Huang, "Solid state transformer in the future smart electrical system," in *Proc. 2013 IEEE Power Energy Soc. Gen. Meeting*, pp.1 - 5
- [9] F. Wang, G. Yao, A. Huang, W. Yu, and X. Ni, "A 3.6kV high performance solid state transformer based on 13kV SiC MOSFET," in *Proc. 2014 Power Electronics for Distributed Generation Systems (PEDG)*, pp. 1 - 8
- [10] J. Shi, W. Gou, H. Yuan, T. Zhao, and A. Q. Huang, "Research on voltage and power balance control for cascaded modular solid-state transformer," *IEEE Trans. Power Electron.*, vol. 26, no. 4, pp.1154 - 1166, 2011
- [11] Q. Song, W. Sheng, L. Kou, D. Zhao, Z. Wu, H. Fang, Hengfu Fang, "Smart substation integration technology and its application in distribution power grid," *CSEE Journal of Power and Energy Systems*, vol. 2, no. 4, pp.31 -36, 2016
- [12] S. Bifaretti, P. Zanchetta, A. Watson, L. Tarisciotti, and J. Clare, "Advanced power electronic conversion and control system for universal and flexible power management," *IEEE Trans. Smart Grid*, vol. 2, no. 2, pp. 231 - 243, Jun. 2011.
- [13] T. Zhao, J. Zeng, S. Bhattacharya, M. E. Baran, and A. Q. Huang, "An average model of solid state transformer for dynamic system simulation," in *Proc. 2009 IEEE Power Energy Soc. Gen. Meeting*, pp.1 - 8
- [14] F. Gao, Z. Li, P. Wang, F. Xu, Z. Chu, Z. Sun, and Y. Li, "Prototype of smart energy router for distribution DC grid," in *Proc. 2015 Power Electronics and Applications (EPE'15 ECCE-Europe)*, pp. 1 - 9
- [15] S. Lu, Z. Zhao, J. Ge, L. Yuan, and T. Lu, "A new power circuit topology for energy router," in *Proc. 2014 IEEE International*

Conference on Electrical Machines and Systems (ICEMS), pp.1921 - 1925.

- [16] A. Sanchez-Squella, R. Ortega, R. Grino, and S. Malo, "Dynamic energy router," *IEEE Control Systems*, vol. 30, no. 6, pp. 72 - 80, 2010.
- [17] X. Guo, H. Wang, Z. Lu. "New inverter topology for ground current suppression in transformerless photovoltaic system application". *Journal of Modern Power Systems and Clean Energy*, vol. 2, no. 2, pp. 191-194, 2014.
- [18] F. Wang, A. Huang, G. Wang, X. She and R. Burgos, "Feed-forward control of solid state transformer," in *Proc. 2012 IEEE, Applied Power Electronics Conference and Exposition (APEC)*, pp. 1153 - 1158
- [19] Q. Duan, C. Ma, W. Sheng, and C. Shi, "Research on power quality control in distribution grid based on energy router," in *Proc. 2014 Power System Technology (POWERCON)*, pp.2115 - 2121
- [20] J. Cao and M. Yang, "Energy internet - towards smart grid 2.0," in *Proc. 2013 Fourth International Conference on Networking and Distributed Computing (ICNDC)*, pp.105 - 110
- [21] L. Chen, Q. Sun, L. Zhao and Q. Cheng, "Design of a novel energy router and its application in energy internet," in *Proc. 2015, Chinese Automation Congress (CAC)*, pp. 1462 - 1467
- [22] Y. Deng, G. Venayagamoorthy and R. Harley, "Optimal allocation of power routers in a STATCOM-installed electric grid with high penetration of wind energy," in *Proc. 2015, Power Systems Conference (PSC)*, pp. 1 - 6
- [23] C. Gu, Z. Zheng and Y. Li, "Control strategies of a multiport power electronic transformer (PET) for DC distribution applications," in *Proc. Electric Ship Technologies Symposium (ESTS), 2015 IEEE*, pp. 135 - 139
- [24] J. Yan, X. Zhu and N. Lu, "Smart hybrid house test systems in a solid-state transformer supplied microgrid," in *Proc. 2015 IEEE Power Energy Soc. Gen. Meeting*, pp.1 - 5
- [25] L. Yuan, S. Wei, J. Ge, Z. Zhao and R. Huang, "Design and implementation of AC-DC hybrid multi-port energy router for power distribution networks," in *Proc. 2015, Electrical Machines and Systems (ICEMS)*, pp. 591 - 596
- [26] M. McDonough, "Integration of inductively coupled power transfer and hybrid energy storage system: a multiport power electronics interface for battery-powered electric vehicles," *IEEE Trans. Power Electron.*, vol. 30, no. 11, pp. 6423 - 6433, 2015.
- [27] X. Zhou, F. Wang and Y. Ma, "An overview on energy internet," in *Proc. Mechatronics and Automation (ICMA), 2015 IEEE International Conference on*, pp. 126 - 131.
- [28] J. Miao, N. Zhang and C. Kang, "Generalized steady-state model for energy router with applications in power flow calculation," in *Proc. 2016 IEEE Power Energy Soc. Gen. Meeting*, pp.1 - 5
- [29] Y. Yuan, P. Li, X. Kong, J. Liu, Q. Liu and Y. Wang, "Harmonic influence analysis of unified power flow controller based on modular multilevel converter". *Journal of Modern Power Systems & Clean Energy*, vol. 4, no. 1, pp. 10 - 18, 2016.
- [30] Y. Pipelzadeh, B. Chaudhuri, T. Green, Y. Wu, H. Pang and J. Cao, "Modelling and dynamic operation of the Zhoushan DC grid: world's first five-terminal VSC-HVDC project" in *Proc. 2015 International High Voltage Direct Current 2015 Conference*. pp. 87 - 95.
- [31] G. Tang, H. Pang, Z. He, "R&D and application of advanced power transmission technology in China" *Proceedings of the CSEE*, vol. 36, no. 7, pp. 1760 - 1771, 2016.
- [32] R. Engelen and W. Zhang, "Security analysis and optimization," in *Proc. Services - Part I, 2008. IEEE Congress on*, pp. 209 - 210
- [33] Z. Yan, N. D. Xiang, B. M. Zhang, S. Y. Wang, and T. S. Chung, "A hybrid decoupled approach to optimal power flow," *IEEE Trans. Power Syst.*, vol. 11, no. 2, pp. 947 - 954, May 1996.
- [34] J. Nocedal, A. Wachter, and R. A. Waltz, "Adaptive barrier strategies for nonlinear interior methods," IBM T.J. Watson Research Center, Yorktown Heights, USA, Tech. Rep. RC 23563, March. 2005.
- [35] A. Wachter and L. T. Biegler, "On the implementation of a primal-dual interior point filter line search algorithm for large-scale nonlinear programming," in *Mathematical Programming*, vol. 106, no. 1, pp. 25 - 57, 2006.
- [36] L. Zhang, L. Harnefors and H. P. Nee, "Interconnection of two very weak AC systems by VSC-HVDC links using power-synchronization control". *IEEE Trans. Power Syst.*, vol. 26, no. 1, pp. 344 - 355, May 2011.



Jianqiang Miao (S'16) was born in Jiangsu Province in China, on December 12, 1992. He received his B.E. degree in electrical engineering from Tsinghua University, China, in 2015.

He is now a master student in electrical engineering in Tsinghua University, China. His research interests include power system load forecasting, energy internet and energy routers.



Ning Zhang (S'10, M'12) received both B.S. and Ph.D. from the Electrical Engineering Department of Tsinghua University in China in 2007 and 2012, respectively.

He is now an Associate Professor at the same university. His research interests include multiple energy system integration, renewable energy, and power system planning and operation (ningzhang@tsinghua.edu.cn).



Chongqing Kang (M'01, SM'07, F'17) received his Ph.D. from the Electrical Engineering Department of Tsinghua University in 1997.

He is now a Professor at the same university. His research interests include power system planning, power system operation, renewable energy, low carbon electricity technology and load forecasting.



Jianxiao Wang (S'14) received the Bachelor's degree in electrical engineering from Tsinghua University, Beijing, China, in 2014, where he is currently pursuing the Ph.D. degree.

His current research interests include power system economics and optimization, power markets, power system scheduling and planning.



Yi Wang (S'14) received the B.S. degree from the Department of Electrical Engineering in Huazhong University of Science and Technology (HUST), Wuhan, China, in 2014.

He is currently pursuing Ph.D. degree in Tsinghua University. His research interests include load forecasting, demand response, and big data applications to smart grid.



Qing Xia (M'01, SM'08) received his Ph.D. from the Electrical Engineering Department of Tsinghua University, China in 1989.

He is now a Professor at the same university. His research interests include electricity markets, generation schedule optimization and power system planning.